Simultaneous crack and temperature sensing with passive patch antenna

Xianzhi Li[1], Songtao Xue[1,2], Liyu Xie[1] and Guochun Wan[3]

Abstract

This article presents a novel passive patch antenna sensor for simultaneous crack and temperature sensing, and the antenna sensor has the ability of temperature self-compensation. The passive patch antenna sensor consists of an underlying patch and an overlapping sub-patch. The off-center feeding activates resonant modes in both transverse and longitudinal directions. The resonant frequency shift in transverse direction is used for environmental temperature sensing, while the structural crack width can be sensed by the longitudinal resonant frequency shift after temperature compensation. Furthermore, the unstressed design of the antenna can also eliminate the issue of incomplete strain transfer ratios. In this article, the relationships between the antenna resonant frequencies, the environmental temperature, and the structural crack width were studied. Simulations were conducted to determine the optimal off-center fed distance of the patch antenna sensor. Furthermore, a series of experimental tests were also conducted, where the passive patch antenna was fabricated and installed on the concrete components as well as an actual building. Continuous monitoring was performed for several days to test the temperature sensing ability of the passive patch antenna, and the sensed crack width after temperature compensation was compared with the actual results. The results of these experiments demonstrate the feasibility of using the passive patch antenna for simultaneous temperature and crack sensing.

Introduction

Structural damages such as cracks will inevitably occur during the long-term service of civil engineering structures. Cracks can be caused by a variety of factors, such as the structural service loads, defects in building materials, and environmental effects. However, such cracks can have serious adverse effects on the structure, reduce the bearing capacity and durability of the structure, or even leading to sudden structural failure and resulting in casualties and property losses. Therefore, it is of great significance to detect the structural cracks promptly to identify the potential structural issues and take necessary measures.[1]

Traditional crack sensing methods such as regular visual inspections with magnifying lens are usually time-consuming and sometimes inaccurate.[2] These laborious crack detection methods are not suitable for modern structural health monitoring. In recent years, sensors play an increasingly important role in structural health monitoring, which can provide more accurate sensing of structural cracks.[3] For example, some piezoelectric-based crack sensors,[4,5] optical fiber-based crack sensors,[6,7] vision-based crack sensors,[8–11]

conductive material-based crack sensors,[12] and acoustic emission-based crack sensors[13,14] have been utilized for structural crack sensing. These sensors make it easier and more accurate to detect structural cracks in real time. However, these crack sensing technologies usually based on wired sensors and need numerous wires for power supply and information transmission, which make it difficult to install and maintain in actual engineering.[15] Furthermore, these crack sensors often affected by environmental temperature changes. When the environmental temperature varies, the sensing of cracks may be inaccurate, or additional temperature

[1]Department of Disaster Mitigation for Structures, Tongji University, Shanghai, China
[2]Department of Architecture, Tohoku Institute of Technology, Sendai, Japan
[3]Department of Electronic Science and Technology, Tongji University, Shanghai, China

Corresponding author:
Liyu Xie, Department of Disaster Mitigation for Structures, Tongji University, Room B508, Building of Civil Engineering, Siping Road 1239, Shanghai 200092, China.
Email: liyuxie@tongji.edu.cn

sensors may be required for measurements correction and compensation.[16] These drawbacks greatly limit the practical use of the crack sensors.

In recent years, passive Internet of Things (IoT) has developed rapidly. Passive IoT refers to a category of passive devices and sensors that do not require batteries or wired power supply, and utilize external energy to transmit and receive data. The implementation of passive IoT is based on technologies such as radio frequency identification (RFID) or near-field communication (NFC), which uses radio waves or electromagnetic fields to transmit sensing data and information. Since the passive sensor does not require batteries or other power sources, it has the advantages of low cost, easy installation, and eliminate the need to replace batteries. Compared with traditional sensors, passive sensors are more suitable for practical applications.

Antenna sensor is a type of passive sensor which does not need power supply and can be interrogated wirelessly. Compared with traditional sensors, the antenna sensor does not need batteries or power sources, and it can be interrogated wirelessly through RFID readers, which makes it easier to integrate with passive IoT as a sensing unit. Therefore, the antenna sensors have great potential in the future structural health monitoring. In past decades, some antenna-based sensors came into being to avoid the defects of traditional sensors.[17–19] The sensing principle of the antenna-based sensor is that the change in monitored physical parameters will lead to the change in electromagnetic parameters of the antenna.[20] Using the antenna itself as the sensor to detect variations in physical parameters, antenna-based sensors offer the benefits of passive and wireless sensing. Furthermore, since the electromagnetic waves of the antenna sensor can penetrate some coverings, the antenna sensor can be used in some embedded or covered situations, making it highly suitable for structural health monitoring. A lot of antenna-based sensors have been developed. For example, Xu and Huang[21] proposed a battery-less and wireless patch antenna sensor for strain sensing; Sanders et al.[22] proposed a microstrip patch antenna for temperature sensing; Zhou et al.[23] proposed an antenna sensor for concrete humidity monitoring; Xue et al.[24] proposed a patch antenna-based bolt loosening sensor; Yi et al.[25,26] proposed a patch antenna sensor for cement hydration setting time detection; and so on.

In terms of structural crack sensing, some antenna-based crack sensors have developed rapidly in recent years.[27] Yi et al.[28,29] proposed a patch antenna for crack sensing, and simulations and experimental tests are conducted to demonstrate that the sensor can detect the small crack on the structure surface. However, the proposed crack sensor based on monolithic patch

antenna need to be attached to the structure's surface and stressed, leading to potential issues such as incomplete strain transfer and insufficient bonding strength.[30] This problem greatly limits the monolithic patch antenna-based crack sensor use in practice. In this regard, Xue et al.[31–33] proposed an unstressed patch antenna sensor to avoid the problem of incomplete strain transfer ratio, which can detect the cracks or structural deformation by the relative movement between two antenna components, making the measurements of structural deformation and crack width more accurate. However, these crack sensors only focus on crack sensing while disregarding the effects of environmental temperature. In actual engineering, the environmental temperature is not constant; thus, the temperature fluctuation will generate inaccurate measurements. To improve the sensing performance of antenna-based crack sensors under variable temperatures, the temperature effects on antenna should be investigated, and additional temperature sensors are needed to measure the environmental temperature for the compensation of the monitored parameters.[34–37]

Since the additional temperature sensors will bring a lot of trouble in practice, to avoid the additional temperature compensation sensors, some scholars have studied the environmental temperature effect on antenna and proposed some methods to eliminate the influence of temperature. For example, Li et al. proposed a thermally stable patch antenna sensor for strain and crack sensing. The use of the thermally stable substrate can avoid the influence of temperature on antenna sensors since the relative dielectric constant of the thermally stable substrate does not change significantly in the case of temperature fluctuation. However, the thermally stable substrate is usually more expensive.[34] Besides, the temperature itself is also a parameter that should be monitored in structural health monitoring. Tchafa and Huang[38] proposed a patch antenna sensor which can simultaneously measure the environmental temperature and the dielectric constant of the medium above the sensor. This multiple physical variable monitoring sensor enabled dielectric constant and temperature sensing by a single antenna sensor, eliminating the need for additional temperature sensors. Li et al.[39] proposed a dual-resonant patch antenna to detect the crack width and temperature changes, which is the preliminary work of this article. The antenna sensor has been proved to be feasible in laboratory environment. However, the temperature compensation mechanism of the antenna sensor and the sensing performance test in actual building and continuous monitoring of the temperature and crack width still need further study. Tchafa and Huang[40] also decouple the effect of temperature and strain on antenna and proposed a sensor capable of
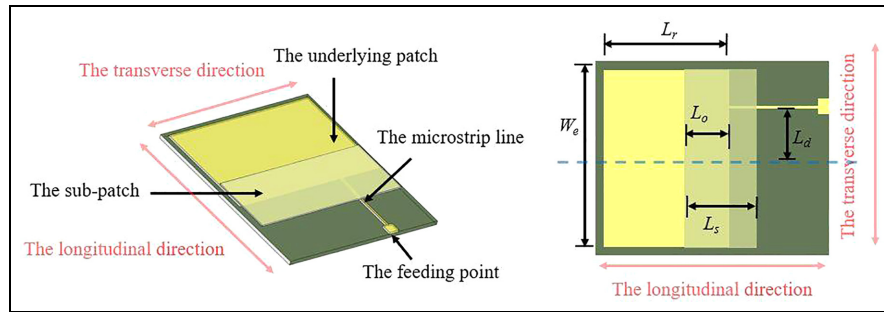
Figure 1. The patch antenna sensor for environmental temperature and structural crack sensing.

simultaneously detecting strain and temperature. However, this sensor is still based on the monolithic antenna and cannot avoid the problem of incomplete strain transfer ratio when used for crack sensing.

In this article, we developed a passive patch antenna sensor for simultaneous crack and temperature sensing, and a series of experimental tests are conducted to demonstrate its actual performance. The proposed passive patch antenna sensor comprises an off-center fed underlying patch and a sub-patch that overlaps it. The underlying patch is fixed, the sub-patch is attached to the it and moves as the crack width changes. The off-center feeding can activate the integrated patch antenna resonant modes in both transverse and longitudinal directions, and the resonant frequency shifts in two directions are used for environmental temperature sensing and structural crack sensing, respectively. Theoretical analysis is conducted to study the relationships between the antenna resonant frequencies, the environmental temperature, and the crack width. The temperature compensation mechanism and the relationship between the off-center fed distance and two resonant modes of the antenna are also studied. To further demonstrate the effectiveness and feasibility of the proposed sensor, some experimental tests were conducted. The patch antenna sensor was fabricated and installed on the concrete components, and several days of continuous monitoring obtained a series of measurements under different environmental temperatures. The experimental results show that the sensor can accurately measure the environmental temperature and structural crack width changes. Furthermore, the proposed patch antenna sensor was also installed in an actual building and tested the performance, which is a meaningful test for the actual use of the patch antenna sensor.

The rest of the article is organized as follows. First, the methodology and theoretical analysis of the proposed patch antenna sensor are introduced. Then, simulations of the patch antenna are conducted in high-frequency structure simulator (HFSS) and the

optimal off-center fed distance of the antenna is studied. In the experimental study section, the experimental design and the results of the patch antenna sensor for environmental temperature and structural crack sensing are presented, as well as the measurements in an actual structure. Finally, the conclusion and further research potential of the proposed antenna sensor are discussed.

Methodology and theoretical analysis

Concept of the patch antenna sensor and temperature compensation method

The patch antenna sensor for environmental temperature and structural crack sensing is depicted in Figure 1. The underlying patch is off-center fed and partially overlapped by a sub-patch. They are tightly attached to enable the electric current induced by interrogation electromagnetic waves flow throughout the integrated patch. The antenna has dual-resonance capabilities due to the off-center feeding of the patch antenna, which activates resonant modes in both transverse and longitudinal directions, resulting in two fundamental resonant frequencies. The transverse fundamental resonant frequency of the patch antenna is only influenced by changes in environmental temperature. However, the longitudinal resonant frequency of the patch antenna is influenced by both the environmental temperature and the overlapped length of the sub-patch.

The patch antenna sensor is installed on the surface of the structure, as depicted in Figure 2. A connecting rod links the sub-patch to the fixed plate, with the underlying patch being fastened to one side of the crack and the fixed plate being fixed to the opposite side. Any changes in the crack width will result in relative movement between the underlying patch and the overlapping sub-patch. The sensing of the structural crack width can be accomplished by measuring the relative movement between the two patches. The relative movement between the two patches will lead to the
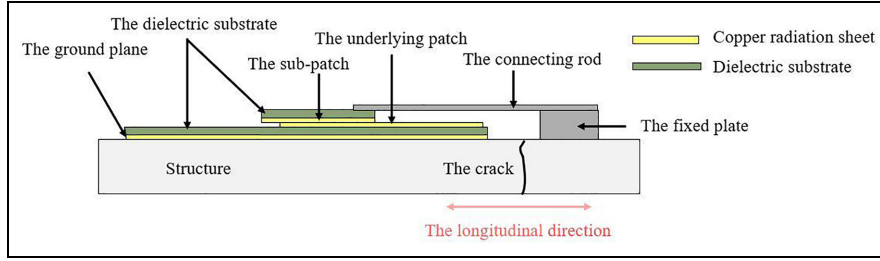
Figure 2. The installation diagram of the patch antenna sensor.

longitudinal length variation of the integrated patch, which will affect the longitudinal resonant frequency of the antenna. Thus, the shift in longitudinal resonant frequency of the antenna can be utilized to measure changes in structural crack, while the shift in transverse resonant frequency is utilized for environmental temperature sensing.

Theoretical analysis of the patch antenna resonant frequency

According to the cavity model theory, the integrated patch of the antenna sensor can be treated as a resonant cavity, and the fundamental resonant frequency of the patch antenna in two directions can be determined as:

$$
f_{10} = \frac{c}{2\pi\sqrt{\varepsilon}} \sqrt{\left(\frac{\pi}{L_e}\right)^2} = \frac{c}{2L_e\sqrt{\varepsilon}} \qquad f_{01} = \frac{c}{2\pi\sqrt{\varepsilon}} \sqrt{\left(\frac{\pi}{W_e}\right)^2}
$$
$$
= \frac{c}{2W_e\sqrt{\varepsilon}}
$$

(1)

where f_{10} represents the fundamental resonant frequency when the patch antenna is resonant at the longitudinal direction and f_{01} represents the fundamental resonant frequency at the transverse direction; c is the speed of light in a vacuum; ε is the relative dielectric constant of the dielectric substrate; and L_e and W_e are the longitudinal electric length and transverse electric length, respectively.

Since the underlying patch and the overlapping sub-patch are tightly attached forming an integrated radiation patch, the electrical length L_e can be calculated:

$$
L_e = L_r + L_s - L_o - \Delta L_o
$$

(2)

where L_r is the radiation sheet length of the underlying patch, L_s is the radiation sheet length of the sub-patch, L_o is the overlapped length between the two patches radiation sheet. ΔL_o is the overlapped length change of the patch antenna, and it is equal to the change in the crack width since the extension of structural crack will

lead to the relative movement between the two patches of the antenna.

When the environment temperature changes ΔT, the variation of temperature will have an impact on the integrated radiation patch size of the patch antenna and the relative dielectric constant of the dielectric substrate, leading to changes in the two fundamental resonant frequencies of the patch antenna sensor. These temperature-related effects can be evaluated from two perspectives: the thermal expansion of the patch antenna and the fluctuations in the relative dielectric constant of the dielectric substrate. The relevant equations are shown as follows:

$$
\Delta\varepsilon_e = k\varepsilon_e\Delta T
$$

(3)

$$
\Delta L_T = \frac{\alpha_{d,1}\Delta TL_r E_{d,1}h_d + 2\alpha_c\Delta TL_r E_c h_c}{2(E_{d,1}h_d + 2E_c h_c)}
$$
$$
+ \frac{\alpha_{d,1}\Delta TL_s E_{d,1}h_d + \alpha_c\Delta TL_s E_c h_c}{2(E_{d,1}h_d + E_c h_c)}
$$

(4)

$$
\Delta W_T = \frac{\alpha_{d,w}\Delta TW_e E_{d,w}h_d + 2\alpha_c\Delta TW_e E_c h_c}{E_{d,w}h_d + 2E_c h_c}
$$

(5)

where $\Delta\varepsilon_e$ represents the relative dielectric constant variation of the dielectric substrate due to the temperature variation, and k is the thermal coefficient corresponding to the dielectric substrate. ΔL_T is the radiation patch size variation in longitudinal direction caused by thermal expansion, while ΔW_T is the size variation in transverse direction caused by thermal expansion. They are related to the material parameters of antenna dielectric plate and radiation sheet, such as thermal coefficients of the dielectric substrate in transverse direction $\alpha_{d,w}$ and in longitudinal direction $\alpha_{d,1}$, the Young's modulus of the dielectric substrate in transverse direction $E_{d,w}$ and in longitudinal direction $E_{d,1}$, the dielectric substrate's height h_d and the copper radiation sheet's height h_c, the thermal expansion coefficient of the copper radiation sheet α_c, and the Young's modulus of the copper sheet E_c.

Based on Equations (1)–(5), when the environmental temperature changes ΔT and the crack width changes

Table 1. The critical dimensions of the patch antenna sensor.

Parameters	W_e (mm)	L_r (mm)	L_s (mm)	L_o (mm)	h_d (mm)	h_c (mm)
Dimensions	51	36	13	9.0	0.51	0.07

ΔL_o, the antenna's fundamental resonant frequencies can be represented as:

$$f_{10}(\Delta T, \Delta L_o) = \frac{c}{2(L_e + \Delta L_T - \Delta L_o)\sqrt{\varepsilon_e + \Delta\varepsilon_e}}$$
$$\approx f_{10} + \frac{\partial f_{10}}{\partial T} \cdot \Delta T + \frac{\partial f_{10}}{\Delta L_o} \cdot \Delta L_o \quad (6)$$

$$f_{01}(\Delta T, \Delta L_o) = \frac{c}{2(W_e + \Delta W_T)\sqrt{\varepsilon_e + \Delta\varepsilon_e}} \approx f_{01} + \frac{\partial f_{01}}{\partial T} \cdot \Delta T \quad (7)$$

According to Equations (6) and (7), both environmental temperature changes and crack width changes can affect the longitudinal resonant frequency, whereas only temperature affects the transverse direction resonant frequency. Therefore, the environmental temperature can be determined by utilizing the resonant frequency shift in the transverse direction, and the temperature compensation for the longitudinal resonant frequency can be calculated simultaneously. Subsequently, the resonant frequency shift in the longitudinal direction of the antenna can be used for the crack width sensing. The sensitivities k_1 and k_2 are defined as the temperature sensitivity in transverse and longitudinal resonant frequencies, and k_3 is defined as the crack sensitivity in longitudinal resonant frequency. The corresponding equations are shown as follows:

$$k_1 = \frac{\partial f_{01}}{\partial T} \quad k_2 = \frac{\partial f_{10}}{\partial T} \quad k_3 = \frac{\partial f_{10}}{\Delta L_o} \quad (8)$$

$$\Delta T = \frac{\Delta f_{01}}{k_1} \quad (9)$$

$$\Delta L_o = \frac{\Delta f_{10}}{k_3} - \frac{\Delta f_{01}}{k_1 k_3} k_2 \quad (10)$$

The calculated ΔL_o according to Equation (10) is the crack width change with temperature compensation. To illustrate the feasibility of the proposed antenna sensor for structural crack and environmental temperature sensing, the theoretical calculation and analysis were carried out. The antenna sensor proposed in this article uses Rogers RT/duroid 5880 laminate with a relative dielectric constant of 2.2 as the dielectric substrate of the patch antenna. The material of the radiation sheet was chosen as copper. The fundamental resonant frequencies of the patch antenna were designed to be approximately 1.95 and 2.5 GHz in the

transverse and longitudinal directions, respectively. According to the commonly used standard thickness of the laminate substrate and the standard thickness of the copper coating, the dielectric substrate's height h_d is determined as 0.51 mm, and the copper radiation sheet's height h_c is determined as 0.07 mm. The antenna size can be determined according to the relative dielectric constant of the dielectric substrate and the Equations (1) and (2). Since the designed resonant frequencies are 1.95 and 2.5 GHz in two directions of the patch antenna, the size of patch antenna in transverse direction W_e and longitudinal direction L_e are calculated as 51 and 40 mm, respectively, based on Equation (1). The radiation sheet length of the underlying patch L_r, the radiation sheet length of the subpatch L_s, and the overlapped length between the two sheets L_o are determined based on Equation (2), since the combined length of these two radiation sheets is equal to the longitudinal length of antenna L_e. The critical dimensions of the patch antenna sensor are shown in Table 1.

Based on Equations (1)–(7), the relationship between the environmental temperature variation, the crack width changes, and the resonant frequencies in two directions can be calculated. Figures 3 and 4 display the resonant frequency shift in transverse direction and longitudinal direction caused by the temperature change from 0°C to 50°C. The corresponding temperature sensitivities are 0.088 MHz/°C and 0.131 MHz/°C, respectively. When the structural crack width changes from 0 to 3 mm, the resonant frequency shift in longitudinal direction is shown in Figure 5, and the crack sensing sensitivity is 63.3 MHz/mm. The resonant frequency shifts in two directions of the antenna both show a good linear trend with the change in monitored variable.

Optimal off-center fed distance

According to previous studies, when the antenna is fed from the center of the transverse direction of the radiation patch by microstrip line, only the longitudinal resonant mode can be activated.[17,31] In this regard, the off-center feeding can solve this problem and activate resonant modes in both transverse and longitudinal directions. To further study the optimal off-center fed distance of the proposed patch antenna sensor, the antenna is modeled in HFSS and a series of
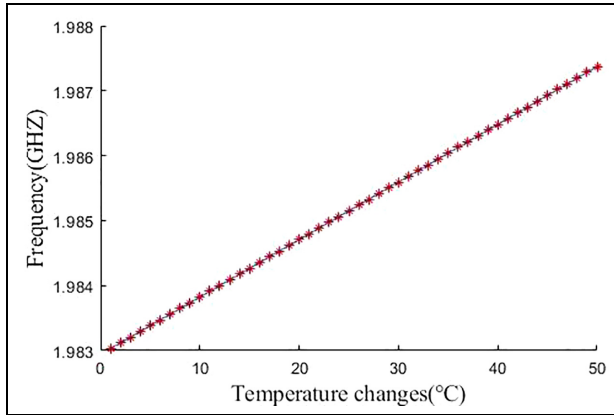
Figure 3. The temperature variation and resonant frequency in transverse direction.
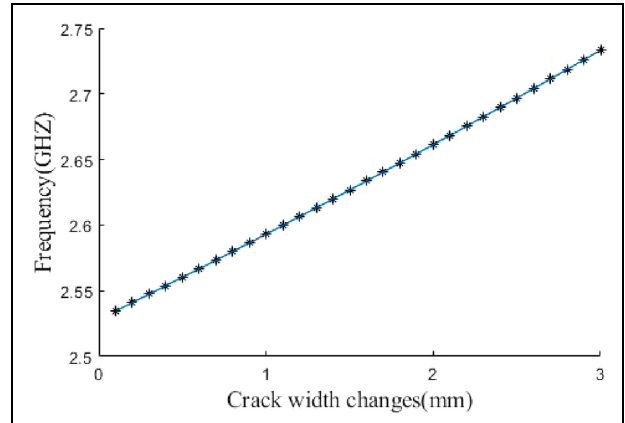

Figure 5. The crack width variation and resonant frequency in longitudinal direction.
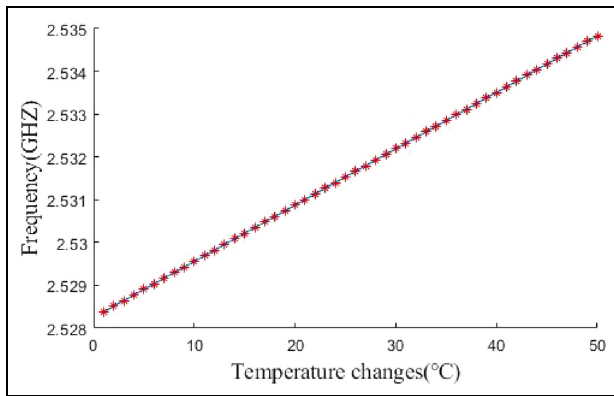

Figure 4. The temperature variation and resonant frequency in longitudinal direction.

Figure 6. The patch antenna modeled in HFSS.
HFSS: high-frequency structure simulator.

simulations were conducted to study the off-center fed distance and the resonant mode.

The off-center fed patch antenna was modeled in HFSS, as shown in Figure 6. The dimensions and materials of the underlying patch and the sub-patch are shown in the previous section. To accurately compute the far-field radiation, the patch antenna was enclosed within an air-box that was a quarter wavelength larger than the antenna size. The patch antenna was excited through a lumped port, and the sweep type was set as interpolating with 4001 sweep points. The frequency range for the sweep was set from 1 to 3 GHz.

According to the theory of antenna and transmission line, the reflection loss curve S_{11} of the patch antenna can be can be determined by Equations (11)–(13):

$$\Gamma = \frac{Z_L - Z_0}{Z_L + Z_0} \tag{11}$$

$$RL(dB) = 10 * \log\left(\frac{P_{in}}{P_{re}}\right) = 10 * \log\left(\frac{V_{in}}{V_{re}}\right)^2$$
$$= 10 * \log\left(\frac{1}{|\Gamma|}\right)^2 = -20 * (|\Gamma|) \tag{12}$$

$$S_{11}(dB) = -RL(dB) \tag{13}$$

where Γ represents the reflection coefficient at the port of the antenna, Z_L represents the port impedance of the antenna, Z_0 represents the impedance of the transmission line, and the standard impedance of the
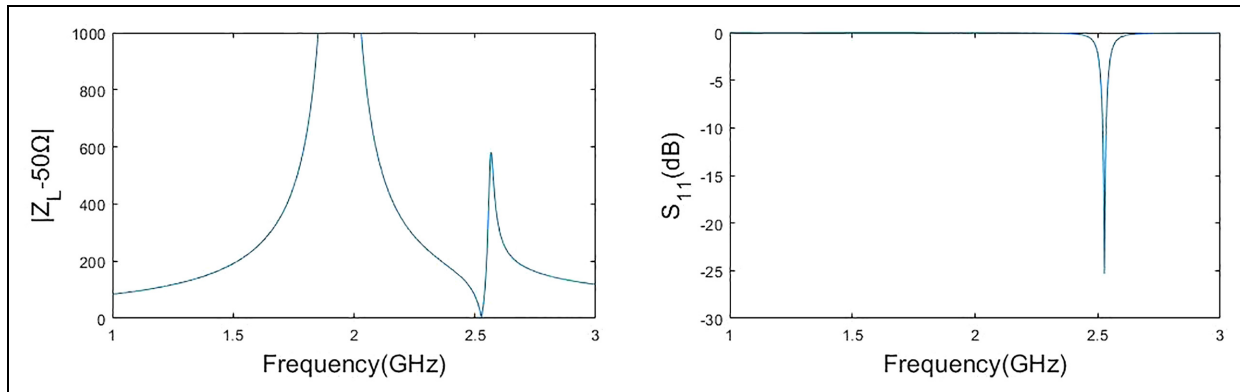
Figure 7. The impedance curve and the S11 curve of the patch antenna (L_d = 0 mm).

transmission line is 50 Ω. RL is the return loss coefficient of the antenna, which is related to the ratio of incident voltage V_{in} to reflected voltage V_{re} at the antenna port. P_{in} and P_{re} represent the incident power and reflected power at the antenna port, respectively. Thus, when the port impedance of the antenna is close to 50 Ω, the impedance matching is good, the ratio of incident power to reflected power is large and the return loss coefficient is large, the minimum value of S_{11} curve is far away from 0 dB, and the resonant mode is significantly excited. On the contrary, when the impedance is not matched, the ratio of incident power to reflected power is close to 1, the return loss coefficient is very small, and the S_{11} curve is near 0 dB, which indicates that the resonant mode is almost not excited.

Figure 7 shows the impedance curve and the reflection loss curve S_{11} of the patch antenna when the antenna is fed from the center of the transverse direction, that is, when $L_d = 0$. It can be seen that the port impedance of the antenna is much larger than 50 Ω around 1.95 GHz, so the transverse resonant mode of the antenna cannot be excited. The S_{11} curve of the patch antenna also shows that only the longitudinal resonant mode was excited since there is only a resonant peak around 2.5 GHz. The frequency which corresponds to the minimum points of the curve around 2.5 GHz is the resonant frequency of the patch antenna in the longitudinal direction.

To activate the transverse resonant mode of the patch antenna around 1.95 GHz, off-center feeding is adopted. The key to activate the transverse resonant mode of the antenna is to make the port impedance of the antenna around 1.95 GHz match with 50 Ω as much as possible. Therefore, simulation study was conducted to study the relationship between the off-center fed distance L_d and the antenna port impedance Z_L.
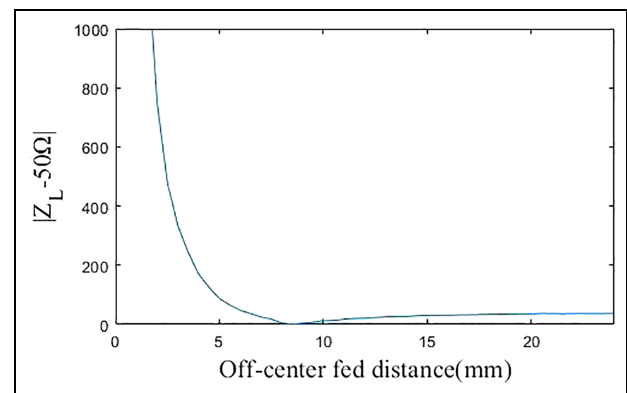

Figure 8. The $|Z_L - 50\,\Omega|$ value under different off-center fed distance.

The off-center fed distance was set to vary from 0 to 24 mm in the simulation, and the increment was set as 0.5 mm. Figure 8 shows the $|Z_L - 50\,\Omega|$ minimum value around 1.95 GHz under different off-center fed distance.

It can be seen that the $|Z_L - 50\,\Omega|$ value varies with the off-center fed distance. The $|Z_L - 50\,\Omega|$ value first decreases and then increases as the off-center fed distance increases from 0 to 24 mm. When the off-center fed distance is 8.5 mm, the $|Z_L - 50\,\Omega|$ minimum value around 1.95 GHz is close to zero, indicating that the impedance match is good and the transverse resonant mode of the antenna is well excited. Thus, the optimal off-center fed distance of the proposed patch antenna sensor is 8.5 mm. The corresponding impedance curve and the reflection loss curve S_{11} of the patch antenna when $L_d = 8.5$ mm are shown in Figure 9. The two resonant peaks around 1.95 and 2.5 GHz also show
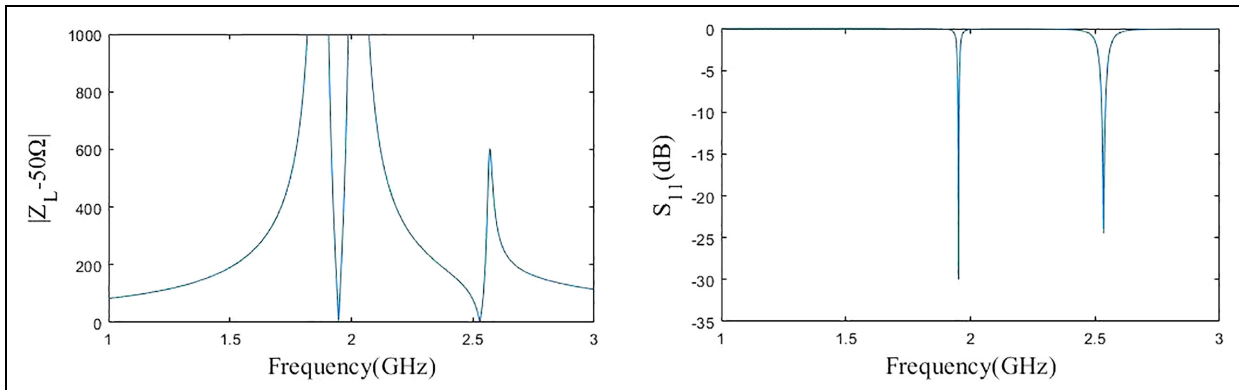
Figure 9. The impedance curve and the S_{11} curve of the patch antenna(L_d = 8.5 mm).

Figure 10. The fabricated patch antenna sensor.
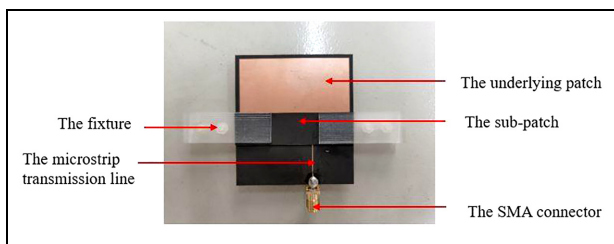

Figure 11. The S_{11} curve of the fabricated patch antenna sensor.

that the resonant mode in both transverse and longitudinal directions are well excited.

Experimental study

The proposed patch antenna sensor dimensions and the off-center fed distance have been determined by theoretical analysis and simulations. In this section, the chemical etching technique was utilized to fabricate the patch antenna sensor, and a series of experiments tests were conducted. Rogers RT/duroid 5880 (https://www.rogerscorp.com) copper clad laminate was cut to the desired size, and then the transmission line and patch shapes were designed and printed onto the laminate using a thermal transfer printer and toner. The laminate coated with toner was then submerged in a corrosive liquid to etch away the unwanted copper. After the etching process, the toner layer covering the patch was removed, the microstrip transmission line was soldered with an subminiature A (SMA) connector. The fabricated patch antenna sensor is shown in Figure 10, and the measured S_{11} curve of the patch antenna sensor is shown in Figure 11. There are two resonant peaks which corresponding to the resonant frequencies in transverse and longitudinal directions, respectively.
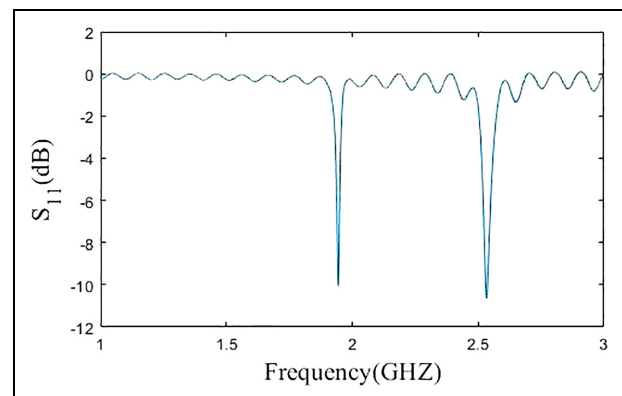
To test the sensing performance of the proposed sensor, a series of experimental tests were carried out. First, the patch antenna sensor was installed on a stationary position in the room to monitor the environmental temperature changes over a period of time utilize the transverse resonant frequency shift. Figure 12 illustrates the experimental setup. The patch antenna sensor was fixed by the fixture. The ground plane of the antenna sensor was pasted on the fixture to maintain the position of the underlying patch, and the sub-patch of antenna sensor was clamped by a fixture. The fixture allows the sub-patch of the antenna to move along the longitudinal direction only when the sub-patch was pushed by the connecting rod. Since there was no connection rod to push the sub-patch to move in the temperature sensing experiment, the presence of the fixture can limit the relative movement between the sub-patch and the underlying patch. Thus, we can focus on the resonant frequency shift of the antenna sensor under the condition of temperature change. The antenna
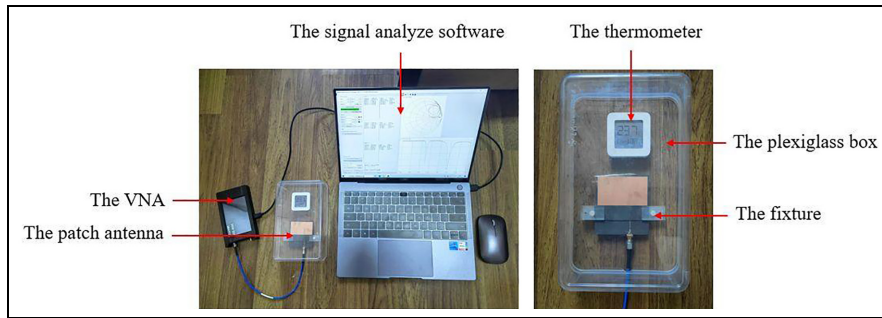
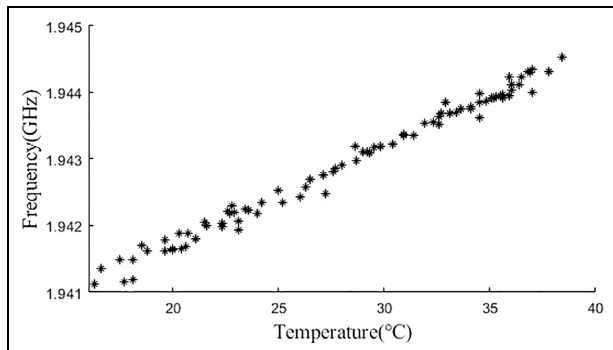**Figure 12.** The experimental setup for temperature sensing and details of the fixture.

Figure 13. The resonant frequency in the transverse direction under different temperature.
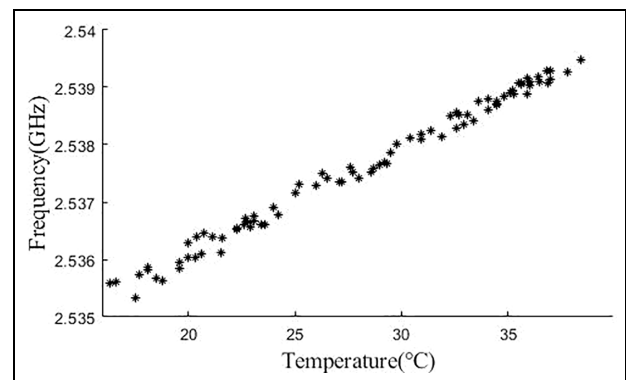

Figure 14. The resonant frequency in the longitudinal direction under different temperature.

sensor was housed within a plexiglass protective box to prevent the interference from dust or other factors during long-term monitoring. A thermometer was placed close to the patch antenna sensor to record the environmental temperature so as to compare with the patch antenna sensor's measurements. The patch antenna sensor in the plexiglass box was connected to the Nano VNA (Vector network analyzer) using a coaxial cable, and the VNA can get the return loss curve S_{11} of the antenna and then obtain the resonant frequency information. In this experiment, the sweeping range of the VNA was set as 1 to 3 GHz, and the number of the sweep points were set as 5050 points.

Continuous monitoring was performed for several days to demonstrate the sensing capability of the patch antenna sensor for long-term environmental temperature monitoring. During the monitoring process, the sunlight sometimes causes the environmental temperature around the antenna to change rapidly, which will affect the accuracy of sensing. Therefore, when recording experimental data, it is necessary to avoid sudden sunlight exposure. To obtain accurate resonant frequency values, the S_{11} curves of the patch antenna were fitted using a quadratic function within the area

surrounding the local minimum point, and the minimum points of the curve around 1.95 GHz is extracted as the resonant frequency in transverse direction. Figure 13 shows some experimental results, it can be seen that the resonant frequency in the transverse direction of the antenna exhibits a correlation with the environmental temperature variation during the monitoring period. The trend can be approximated by linear fitting, and the temperature sensitivity is 0.143 MHz/°C. Figure 14 shows the longitudinal resonant frequency shift corresponding to different temperature. The longitudinal resonant frequency also has a linear relationship with the temperature change, and the sensitivity is 0.184 MHz/°C. Therefore, when the longitudinal resonant frequency of the antenna is used for crack width sensing, the error caused by the temperature change can be compensated by the temperature sensed by transverse resonant frequency and the relationship between the temperature and longitudinal resonant frequency.

To further demonstrate the environmental temperature sensing capabilities, the environmental temperature is recorded several times in a day, and the 24-h environmental temperature changes sensed by the
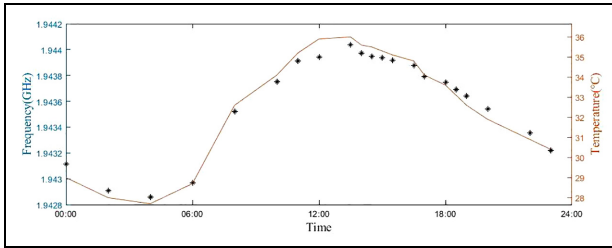
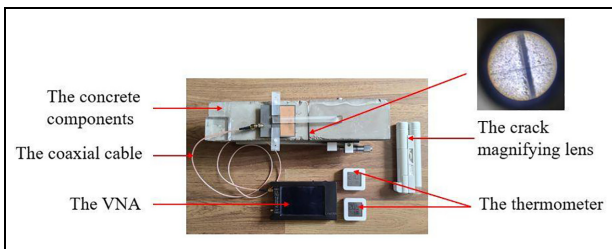**Figure 15.** The 24-h environmental temperature monitoring results.

Figure 16. The top view of the experimental setup.

Figure 17. The side view of the experimental setup.

Figure 18. The experimental setup for structural crack and environmental temperature sensing.

antenna sensor were used to compare with the measurements of the thermometer. The scatter diagram in Figure 15 is the transverse resonant frequency of the patch antenna sensor while the red curve is the environmental temperature recorded by the thermometer. The comparison shows that the temperature curves recorded by the two sensors have a good coincidence, and the error range usually does not exceed 1°C. The experimental results demonstrate that utilizing the transverse resonant frequency shift of the patch antenna for environmental temperature sensing is a feasible method and can be applied to the continuous temperature monitoring.

The patch antenna sensor was also installed on the concrete components to verify the structural crack and environmental temperature sensing capability, shown in Figures 16 and 17. The two concrete components are, respectively, connected to the fixed table through a fixed connection and a moveable fine-tuning table. The concrete components on the moveable table could be pushed by the screw micrometer rod with a precision of 0.01 mm; thus, the two concrete components can move relative to simulate the width changes of structural cracks. When the movable concrete component approached the other concrete component, the crack width decreased. When the two concrete components moved away from each other, the crack width between the two components increased. The screw micrometer rod can accurately measure the relative position change between two concrete components, that is, the change in structural crack width. An 80-time crack magnifying
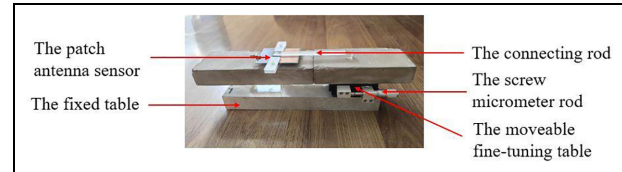
lens with scale was also used to assist in measuring the change of crack width in the experiment, as shown in Figure 16.

The underlying patch of the sensor was glued to the fixed concrete component using a fixture, while the sub-patch was fixed to the other moveable concrete component by a connecting rod. The material used for the connecting rod was selected as glass with a low thermal coefficient of about $8 \times 10^{-6}/°C$. For the connecting rod with a length of 10 cm used in the experiment, the length of the connecting rod will slightly change under temperature changes, approximately 0.0008 mm/°C. Since the value is very small, the influence of thermal expansion of the connecting rod was not considered in this experiment. The patch antenna sensor was connected to the VNA through the coaxial cable to obtain the resonant frequency of the patch antenna sensor. The patch antenna sensor and concrete components were housed in a plexiglass protective box, shown in Figure 18. Two thermometers were placed inside the box and record the environmental temperature variation. The average temperature of the two thermometers is taken as the recorded environmental temperature to reduce the test error.

The screw micrometer rod was used to push the moveable concrete component with an increment of 0.02 mm and the crack width changed accordingly. The experimental tests were conducted under three different environmental temperatures of 15, 20, and 25 °C. The patch antenna sensor's longitudinal resonant frequency varies with the crack width as shown in Figure 19. It can be seen that the longitudinal resonant frequency of the antenna has a linear correlation with the crack width at a constant temperature, and the
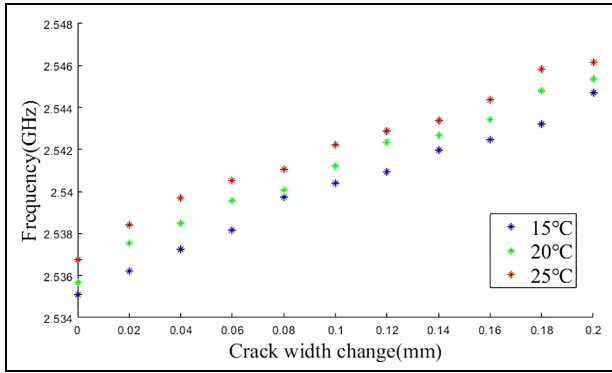
Figure 19. The experimental results under the crack width and environmental temperature change.
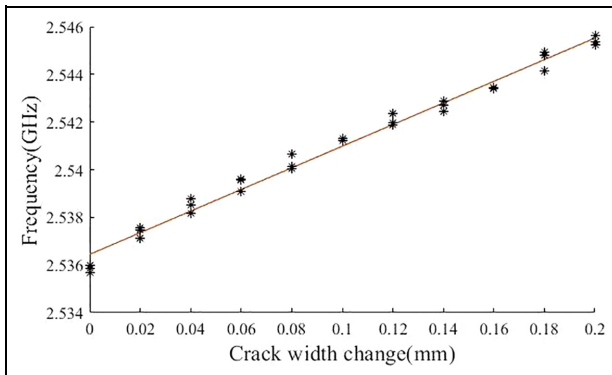

Figure 20. The longitudinal resonant frequency with temperature compensation for crack sensing.

average sensitivity is 45.3 MHz/mm. The changes in environmental temperature will also cause the shift in longitudinal resonant frequency. When the environmental temperature increases, the longitudinal resonant frequency corresponding to the same crack width increases correspondingly, and the temperature sensitivity is 0.187 MHz/°C. Therefore, after the environmental temperature is sensed by the transverse resonant frequency shift, the influence of the temperature variation on the longitudinal resonant frequency can be calculated, thus realizing the temperature self-compensation and structural crack sensing. The longitudinal resonant frequency with temperature compensation for crack sensing is shown in Figure 20.

To verify the feasibility of the proposed patch antenna sensor for structural crack and environmental temperature sensing in practice, the sensor was installed in an actual building to test its performance. The South building of Huadong Hospital is a famous historic building in China, and the building was uplifted to correct the subsidence caused by long-term use in 2021.[41] The uplifting process of the building occurred from August 26 to September 04. In the uplifting and renovation project, the patch antenna sensor developed by the authors was installed and used to monitor the structural cracks and environmental temperature. The experimental test achieved good results.

The South building of Huadong Hospital under renovation is shown in Figure 21. Some structural cracks appeared in this old building after its long-term use, such as the cracks on the wall and roof. During the uplifting process, the uneven vertical displacement of the building sometimes leads to a change in crack width. Therefore, the patch antenna sensors were installed near two structural cracks on the wall and roof, respectively, to measure the change in crack width as well as the environmental temperature, as shown in Figure 22. The conventional structural crack sensor (Figure 18) and thermometer were also installed on the crack to monitor the change in crack width and environmental temperature to compare with the results measured by the patch antenna sensor.

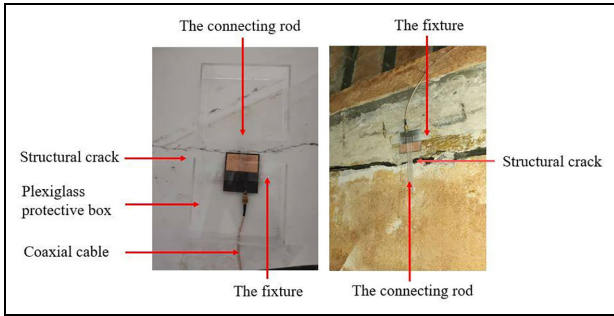**Figure 21.** The building renovation project and the installed patch antenna sensor.

Figure 22. The installation diagram of the patch antenna sensor.

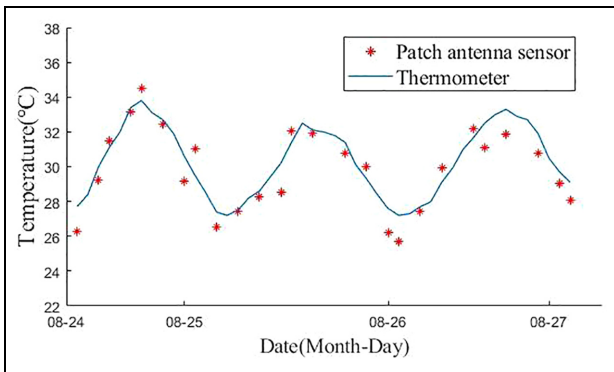**Figure 24.** The crack width measurements with and without temperature compensation.

Figure 23. The temperature measurements comparison.

The patch antenna sensor utilizes the resonant frequency shift in the transverse direction for environmental temperature sensing. First, the initial transverse resonant frequency of the antenna sensor and the environmental temperature should be measured after installation, and then the environmental temperature variation can be calculated according to the shift of the transverse resonant frequency and the temperature sensitivity of the patch antenna sensor. The comparison of the sensed temperature between the patch antenna sensor and the thermometer is shown in Figure 23. The average error of environmental temperature measurement with the patch antenna sensor is 1.12°C. This is mainly due to the interference of the actual engineering environment. The patch antenna sensor is highly sensitive, meaning that even a minor shift in its transverse resonant frequency can indicate a significant variation in environmental temperature. However, due to external factors such as site construction and dust, the transverse resonant frequency of the patch antenna sensor has been slightly interfered, which affects the temperature sensing accuracy of the patch antenna sensor. Therefore, when the patch antenna sensor is used in practical engineering, it needs to be properly
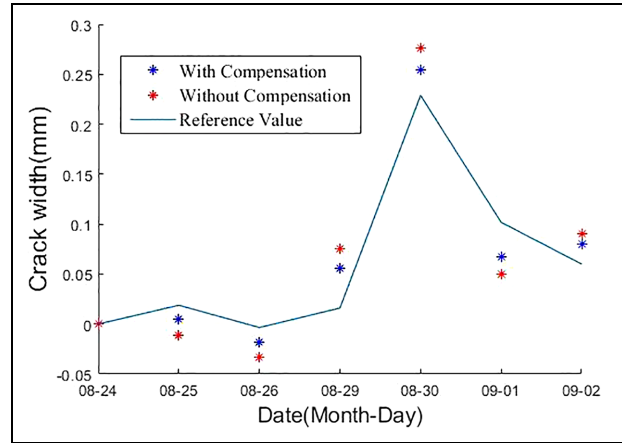
packaged and protected to avoid the interference of dust and other factors.

The measurement principle of the crack sensors is to fix the sensor on both sides of the crack and measure the crack width change. Thus, the initial crack width when the sensor installed was assumed to be zero. Figure 24 shows the measurements of the structural crack on the wall. The blue line is the measured value by conventional wired crack sensor, which serves as the reference value of the crack width. The crack width values measured directly by the antenna longitudinal resonance frequency shift are shown by the red scatters in Figure 24. After temperature compensation, the average error of sensed crack width is obviously reduced from 0.041 to 0.025 mm. The crack width values sensed by the patch antenna after temperature compensation are shown by the blue scatters in Figure 24. The temperature compensated patch antenna sensor measurements show good consistency with the reference values. From the measurements of crack width change, it can be seen that the structural crack width suddenly increased on August 30, and the width of the crack decreased in the subsequent measurement. This is due to the uneven uplifting of the building on August 30, which led to the expansion of cracks. The uneven uplifting was gradually corrected in the subsequent uplifting process, and the crack width also decreased correspondingly. The crack width measurement results were in good agreement with the actual situation of the building.

Conclusions

This article introduced a passive patch antenna sensor and conducted a series of experiments to test its

performance in environmental temperature and structural crack sensing. The patch antenna sensor is off-center fed and dual resonant; thus, the environmental temperature and structural crack can be detected by the patch antenna's resonant frequency shifts in two different directions, respectively. The relationships between the antenna resonant frequencies and the sensed variables were conducted, as well as the simulation study of the optimal off-center fed distance of the proposed patch antenna sensor. A series of experimental tests were conducted, and experimental results demonstrated the feasibility of the proposed antenna sensor. Furthermore, to test the actual performance of the patch antenna sensor, the sensor was used in an actual structural monitoring project. Although the accuracy of measurements on actual buildings still needs to be improved, it is a meaningful test for the actual use of the proposed patch antenna sensor. In future work, significant concerns such as the effective wireless interrogation technique, strategies to overcome interference caused by environmental electromagnetic waves, as well as the approaches to increase wireless interrogation distance of the antenna sensor still need to be further investigated to improve the applicability of the proposed sensor.

Declaration of conflicting interests

Funding

ORCID iDs

Xianzhi Li https://orcid.org/0000-0002-1314-5781
Liyu Xie https://orcid.org/0000-0001-5777-0645

References

1. Taheri S. A review on five key sensors for monitoring of concrete structures. *Constr Build Mater* 2019; 204: 492–509.
2. Chang Q, Yang W, Liu J, et al. A research on fatigue crack growth monitoring based on multi-sensor and data fusion. *Struct Health Monit* 2021; 20: 848–860.
3. Yao Y, Tung S and Glisic B. Crack detection and characterization techniques-an overview. *Struct Control Health Monit* 2014; 21(12): 1387–1413.
4. Wang T, Tan B, Lu M, et al. Piezoelectric electromechanical impedance (EMI) based structural crack monitoring. *Appl Sci* 2020; 10(13): 4648.
5. Kocherla A, Duddi M and Subramaniam K. Embedded PZT sensors for monitoring formation and crack opening in concrete structures. *Measurement* 2021; 182: 109698.
6. Ou R, Luo L and Soga K. Brillouin scattering spectrum-based crack measurement using distributed fiber optic sensing. *Struct Health Monit* 2022; 21(4): 1345–1366.
7. Han T, Wu G and Lu Y. Crack monitoring using short-gauged Brillouin fiber optic sensor. *Measurement* 2021; 179: 109461.
8. Kim H, Lee S, Ahn E, et al. Crack identification method for concrete structures considering angle of view using RGB-D camera-based sensor fusion. *Struct Health Monit* 2021; 20(2): 500–512.
9. Yu Y, Rashidi M, Samali B, et al. Crack detection of concrete structures using deep convolutional neural networks optimized by enhanced chicken swarm algorithm. *Struct Health Monit* 2022; 21(5): 2244–2263.
10. Gong Q, Zhu L, Wang Y, et al. Automatic subway tunnel crack detection system based on line scan camera. *Struct Control Health Monit* 2021; 28(8): e2776.
11. Kong S, Fan J, Liu Y, et al. Automated crack assessment and quantitative growth monitoring. *Comput-Aided Civ Infrastruct Eng* 2021; 36(5): 656–674.
12. Pour-Ghaz M, Barrett T, Ley T, et al. Wireless crack detection in concrete elements using conductive surface sensors and radio frequency identification technology. *J Mater Civ Eng* 2014; 26(5): 923–929.
13. Wang J and Guo J. Damage investigation of ultra high performance concrete under direct tensile test using acoustic emission techniques. *Cem Concr Compos* 2018; 88: 17–28.
14. Bhuiyan M, Bao J, Poddar B, et al. Toward identifying crack-length-related resonances in acoustic emission waveforms for structural health monitoring applications. *Struct Health Monit* 2018; 17(3): 577–585.
15. Zhang J, Tian G, Marindra A, et al. A review of passive RFID tag antenna-based sensors and systems for structural health monitoring applications. *Sensors* 2017; 17: 265.
16. Luo D, Yue Y, Li P, et al. Concrete beam crack detection using tapered polymer optical fiber sensors. *Measurement* 2016; 88: 96–103.
17. Chung K, Wang L, Luo J, et al. Comparative study on directional sensitivity of patch-antenna-based strain sensors. *Int J RF Microwave Comput-Aided Eng* 2020; 30(11): e22398.
18. Wan G, Kang W, Wang C, et al. Separating strain sensor based on dual-resonant circular patch antenna with chipless RFID tag. *Smart Mater Struct* 2021; 30(1): 015007.
19. Huang H, Farahanipad F and Singh A. A stacked dual-frequency microstrip patch antenna for simultaneous shear and pressure displacement sensing. *IEEE Sens J* 2017; 17(24): 8314–8323.
20. Wan G, Li M, Yang Y, et al. Patch-antenna-based structural strain measurement using optimized energy

detection algorithm applied on USRP. *IEEE Internet Things J* 2021; 8(9): 7476–7484.

21. Xu X and Huang H. Battery-less wireless interrogation of microstrip patch antenna for strain sensing. *Smart Mater Struct* 2012; 21(12): 125007.

22. Sanders J, Yao J and Huang H. 2015 Microstrip patch antenna temperature sensor. *IEEE Sens J* 2015; 15(9): 5312–5319.

23. Zhou S, Deng F, Yu L, et al. A novel passive wireless sensor for concrete humidity monitoring. *Sensors* 2016; 16(9): 1535.

24. Xue S, Li X, Xie L, et al. A bolt loosening detection method based on patch antenna with overlapping sub-patch. *Struct Health Monit* 2021; 21(5): 2231–2243.

25. Yi Z, Xue S, Xie L, et al. Detection of setting time in cement hydration using patch antenna sensor. *Struct Control Health Monit* 2021; 29(1): e2855.

26. Yi Z, Xue S, Xie L, et al. A slotted-patch antenna sensor with higher sensitivity for detecting setting time of cement paste. *IEEE Trans Instrum Meas* 2022; 71: 6005513.

27. Caizzone S and DiGiampaolo E. Wireless passive RFID crack width sensor for structural health monitoring. *IEEE Sens J* 2015; 15(12): 6767–6774.

28. Yi X, Cho C, Cooper J, et al. Passive wireless antenna sensor for strain and crack sensing—electromagnetic modeling, simulation, and testing. *Smart Mater Struct* 2013; 22(8): 085009.

29. Cho C, Yi X, Li D, et al. Passive wireless frequency doubling antenna sensor for strain and crack sensing. *IEEE Sens J* 2016; 16: 5725–5733.

30. Xue S, Xu K, Xie L, et al. Crack sensor based on patch antenna fed by capacitive microstrip lines. *Smart Mater Struct* 2019; 28(8): 085012.

31. Xue S, Yi Z, Xie L, et al. A passive wireless crack sensor based on patch antenna with overlapping sub-patch. *Sensors* 2019; 19: 4327.

32. Xue S, Yi Z, Xie L, et al. Double-frequency passive deformation sensor based on two-layer patch antenna. *Smart Struct Syst* 2021; 27(6): 969–982.

33. Xue S, Yi Z, Xie L, et al. A displacement sensor based on a normal mode helical antenna. *Sensors* 2019; 19(17): 3767.

34. Li D and Wang Y. Thermally stable wireless patch antenna sensor for strain and crack sensing. *Sensors* 2020; 20(14): 3835.

35. Sunny A, Zhang J, Tian G, et al. Temperature independent defect monitoring using passive wireless RFID sensing system. *IEEE Sens J* 2019; 19(4): 1525–1532.

36. Fadamiro A, Famoriji O, Zakariyya R, et al. Temperature variation effect on a rectangular microstrip patch antenna. *Int J Online Biomed Eng* 2019; 15(5): 101–118.

37. Djerafi T, Wu K and Deslandes D. A temperature-compensation technique for substrate integrated waveguide cavities and filters. *IEEE Trans Microwave Theory Tech* 2012; 60(8): 2448–2455.

38. Tchafa F and Huang H. Microstrip patch antenna for simultaneous temperature sensing and superstrate characterization. *Smart Mater Struct* 2019; 28(10): 105009.

39. Li X, Xue S, Xie L, et al. An off-center fed patch antenna with overlapping sub-patch for simultaneous crack and temperature sensing. *Smart Mater Struct* 2022; 31(9): 095036.

40. Tchafa F and Huang H. Microstrip patch antenna for simultaneous strain and temperature sensing. *Smart Mater Struct* 2018; 27(6): 065019.

41. Li X, Xie L, Lu W, et al. Structural health monitoring of a historic building during uplifting process: system design and data analysis. *Struct Health Monit*. Epub ahead of print 12 January 2023. DOI: 10.1177759217221135351.